Original article

MOLECULAR METABOLISM

High calorie diet triggers hypothalamic angiopathy

Chun-Xia Yi [a], Martin Gericke [b], Martin Krüger [b], Anneke Alkemade [c], Dhiraj G. Kabra [a], Sophie Hanske [b], Jessica Filosa [d], Paul Pfluger [a], Nathan Bingham [e], Stephen C. Woods [f], James Herman [f], Andries Kalsbeek [g,h], Marcus Baumann [i], Richard Lang [e], Javier E. Stern [d], Ingo Bechmann [b], Matthias H. Tschöp [a,*]

ABSTRACT

Obesity, type 2 diabetes, and related diseases represent major health threats to modern society. Related pathophysiology of impaired neuronal function in hypothalamic control centers regulating metabolism and body weight has been dissected extensively and recent studies have started focusing on potential roles of astrocytes and microglia. The hypothalamic vascular system, however, which maintains the microenvironment necessary for appropriate neuronal function, has been largely understudied. We recently discovered that high fat/high sucrose diet exposure leads to increased hypothalamic presence of immunoglobulin G (IgG1). Investigating this phenomenon further, we have discovered a significant increase in blood vessel length and density in the arcuate nucleus (ARC) of the hypothalamus in mice fed a high fat/high sucrose diet, compared to matched controls fed standard chow diet. We also found a clearly increased presence of α-smooth muscle actin immunoreactive vessels, which are rarely present in the ARC and indicate an increase in the formation of new arterial vessels. Along the blood brain barrier, an increase of degenerated endothelial cells are observed. Moreover, such hypothalamic angiogenesis was not limited to rodent models. We also found an increase in the number of arterioles of the infundibular nucleus (the human equivalent of the mouse ARC) in patients with type 2 diabetes, suggesting angiogenesis occurs in the human hypothalamus of diabetics. Our discovery reveals novel hypothalamic pathophysiology, which is reminiscent of diabetic retinopathy and suggests a potential functional involvement of the hypothalamic vasculature in the later stage pathogenesis of metabolic syndrome.

Keywords Obesity; Diabetes; Blood brain barrier; Capillary; Fluorescent angiography; Endothelial cell

INTRODUCTION

The epidemic of the metabolic syndrome, with obesity and type-2 diabetes at its core, represents one of the most severe health threats of modern society. Based on the outcome of multifaceted research over the last decade, the central nervous system (CNS) has been implicated as the primary organ responsible for pathophysiological processes leading to metabolic syndrome (e.g., obesity induced by leptin resistance) [1–4]. Specific regions of the CNS monitor systemic metabolism, receiving information both from afferent neuronal pathways as well as from signals circulating in the vascular system [5,6]. The arcuate nucleus (ARC) in the mediobasal hypothalamus, adjacent to a circumventricular organ (CVO) median eminence (ME) [7], has a particularly critical role in conveying metabolic information from circulating signals into the neuronal network controlling energy balance. When metabolic feedback to the ARC is impaired, such as in leptin resistance [4], erroneous or misinformed nutrient sensing can result in insufficient, or even counterproductive, responses, exacerbating hyperphagia and metabolic disarray and accelerating the drive toward the metabolic syndrome.

While most studies on the central mechanisms involved in the pathogenesis of the metabolic syndrome have focused on hypothalamic neurons and associated brain regions, emphasis has recently shifted to astrocytes and microglia; the former, the support neuronal growth and energy supply [8], and the latter are responsible for maintaining local homeostatic microenvironments within the CNS. Diet-induced obese mice and rats exhibit astrocytosis and microglial activation in the ARC, as well as loss of anorexigenic pro-opiomelanocortin (POMC) neurons embedded between glial cells [9,10]. Strikingly, high fat/high sucrose (HFHS)-diet induced obese (HFHS-DIO) mice exhibit massive deposition of immunoglobulin G (IgG) that is co-localized with microglia in the ARC-median eminence complex [11], implying that in addition to glial changes that occur during the development of obesity, the vascularization of glial-neuronal networks may also occur.

To investigate whether the hypothalamic vascular system actually undergoes high calorie diet induced structural and functional changes, we applied fluorescent angiography, by injecting fluorescein isothiocyanate conjugated albumin (FITC-albumin), into the general circulation to label the blood vessels. We found an increase of FITC-albumin labeled vessels in the hypothalamus. We then quantified the FITC-albumin labeling vessel profile in the ARC and found an increase in the total length and density of the vessels, characteristics of angiogenesis. To further dissect the profile of this angiogenesis, we performed immunohistochemical staining of arteries and arterioles using α-smooth muscle

[a]Institute for Diabetes and Obesity, Helmholtz Centre for Health and Environment & Technical University Munich, Munich, Germany [b]Institute of Anatomy, University of Leipzig, Germany [c]Cognitive Science Center Amsterdam, University of Amsterdam, Amsterdam, The Netherlands [d]Department of Physiology, Georgia Health Sciences University, Georgia, USA [e]Cincinnati Children's Hospital Medical Center, Cincinnati, USA [f]Institute for Metabolic Diseases, Depts. of Medicine and Psychiatry, University of Cincinnati—College of Medicine, Cincinnati, USA [g]Hypothalamic Integration Mechanisms, Netherlands Institute for Neuroscience, Amsterdam, The Netherlands [h]Department of Endocrinology and Metabolism, Academic Medical Center (AMC), University of Amsterdam, The Netherlands [i]Department of Nephrology, Klinikum rechts der Isar, Technical University Munich, Germany

*Corresponding author.

Received July 21, 2012 • Revision received August 2, 2012 • Accepted August 2, 2012 • Available online Month XX, 2012

http://dx.doi.org/10.1016/j.molmet.2012.08.004

 © 2012 Elsevier GmbH. All rights reserved.

actin (αSMA) [12] in the hypothalami of HFHS-DIO mice. Finally we measured the αSMA immunoreactive vessels in diabetic human hypothalami, where we found a decrease of anorexigenic peptide α-melanocyte-stimulating hormone (αMSH) [13]

MATERIAL AND METHODS

Animals

All studies were approved by and performed according to the guidelines of the Institutional Animal Care and Use Committee (IACUC) of the University of Cincinnati, or in accordance with the German Animal Welfare Act.

Fluorescent angiography study in diet-induced obese mice

Wild-type mice (WT, C57BL/6, n=5) on 18 or 32 weeks of HFHS diet (58% fat with sucrose, Research Diets, D12331, New Brunswick, NJ) (BW: 60.10 ± 3.65 g) and age-matched standard chow (SC)-diet controls (BW: 40.16 ± 0.99 g, n=5) were placed in a restriction tube and received 10 ml/kg of FITC-albumin (MW 69 kDa; Sigma, USA; 10 mg/mL in saline), infused slowly over 5 min. 8 min later, mice were decapitated and brains were immersion-fixed in 4% paraformaldehyde in 0.1 M PBS (pH 7.4) at 4 °C for 72 h. Brains were equilibrated for 48 h with 30% sucrose in 0.1 m Tris-buffered saline (TBS; pH 7.2). Using a cryostat, brains were cut into 30-μm coronal sections, rinsed in 0.1 M TBS, mounted on gelatin-coated glass slides, dried and covered by polyvinyl alcohol mounting medium with DABCO® (Sigma, USA) and visualized by confocal microscopy (Zeiss-LSM710, Germany). For each mouse from the 18-week HFHS and SC-diet groups, we selected two to three sections in the middle portion of the ARC to determine the hypothalamic vessel profile. NeuronJ [14], a program for tracing and quantification of elongated image structures, was used to manually trace the length of FITC-albumin labeled vessels in the ARC, and the mean length from each mouse ARC was calculated. The relative density of vessels inside the ARC was measured by ImageJ with its skeletonization function (NIH, USA).

Time-course of ARC vascular changes on high fat high sucrose diet

Mice were exposed to HFHS diet for 1d or 1, 2, 3, or 18 weeks. 18-week SC-diet fed mice served as age controls (n=8/group). Animals in each group were deeply anesthetized and perfused with saline, followed by a solution of 4% paraformaldehyde in 0.1 M PBS (pH 7.4) at 4 °C. Brains were removed and kept in 4% paraformaldehyde at 4 °C for overnight post-fixation, followed by equilibration of the tissue in TBS containing 30% sucrose before freezing. Using a cryostat, brains were cut into 30-μm coronal sections. To obtain general vessel and arteriole profiles, the immunoreactivity (ir) of αSMA, which labels vascular smooth muscle of arteries and arterioles, pericytes and post-capillary venules [15] was measured in the ARC of respective brain sections. For immunohistochemical labeling, unspecific binding of the antibodies was blocked using 10% normal goat serum followed by incubation with mouse anti-αSMA primary antibodies (1:500; Sigma, USA) at 4 °C over night. After thorough rinsing, sections were then incubated with Alexa488 conjugated goat anti-mouse secondary antibodies (1:200; Life Technologies, Germany) for 1 h, followed by counterstaining with DAPI (Invitrogen, Germany) for 5 min. Sections were rinsed, and cover-slipped using Mowiol mounting medium containing DABCO® (Sigma, USA) and analyzed with an Olympus BX51 fluorescence microscope (Olympus, Germany). For each mouse, four consecutive sections in the middle portion of the ARC were selected and evaluated in a blinded fashion by counting αSMA-ir blood vessels per section.

Electron microscopic analysis of the Blood-brain barrier ultrastructure in diet-induced obese mice

After 18 weeks on HFHS diet, DIO mice and their age-matched SC diet-fed controls were deeply anesthetized and perfused with saline, followed by a solution of 4% paraformaldehyde in 0.1 M PBS (pH 7.4) at 4 °C and 2.5% glutaraldehyde. To process them for electron microscopy, brains were cut into 60-μm sections on a vibrating microtome in phosphate-buffered saline (PBS, pH 7.4). Sections were dehydrated in graded alcohol and stained with OsO_4 and uranyl acetate. After embedding in resin and polymerization for 48 h at 56 °C, the ARC was located in the embedded sections and the blocks were trimmed to prepare ultrathin sections on an ultra-microtome. Ultra-thin sections (55 nm) were collected on Formvar-coated single-slot grids and stained by incubation in lead citrate. Ultrastructural analysis was performed with a Zeiss SIGMA electron microscope (Zeiss, Germany). Ultrastructure of respective vessels was evaluated in an unbiased manner while integrity of tight junctions and the endothelial layer, thickening of basement membranes and peri- or juxtavascular damage served as morphological criteria.

Analysis of vascular profile in postmortem diabetic Human brain tissue

To determine whether the diabetic human hypothalamus has similar vascular changes, we analyzed αSMA-ir vessels in the infundibular nucleus (IFN, equivalent to the ARC) of human brains from diabetic patients.

Human brain material was obtained from The Netherlands Brain Bank at The Netherlands Institute for Neuroscience (Director Dr. I Huitinga) in accordance with formal permissions for brain autopsy and the use of human brain material and clinical information for research purposes. Hypothalami of 10 subjects who had been diagnosed with type 2 diabetes requiring treatment with oral anti-diabetics or insulin, as well as hypothalami of 11 control subjects who were matched for sex, age, and cause of death (i.e., acute or protracted illness) were obtained. For comparison, we also studied two subjects with type 1 diabetes. Clinico-pathological data are presented in supplementary Table 1.

Hypothalami were fixed in 10% phosphate-buffered formalin at room temperature for 4–11 weeks. Post-mortem delay and fixation duration were not different between groups. After dehydration in a series of graded ethanol, tissues were cleared in xylene and embedded in paraffin. Coronal serial sections (6 μm) were cut from the lamina terminalis to the mammillary bodies. Every 100th section was used for Nissl staining for anatomical orientation. αSMA staining was performed on every 100th section of the IFN.

Sections were mounted on Superfrost plus slides and dried for 48 h at 37 °C. After deparaffinization in xylene and rehydration through graded ethanol, sections were washed in Tris buffered saline (TBS, 0.05 M Tris, 0.15 M NaCl, pH7.6) and then incubated in the αSMA primary antibody (Abcam, Cambridge, UK). Dilutions were made in supermix-milk (SUMI-milk 5% nonfat milk, 0.25% gelatin, 0.5% Triton X-100 in TBS, pH 7.6) overnight at 4 °C in a humidified chamber. Sections were pre-incubated in TBS containing 5% milk for 1 h at room temperature to block unspecific binding of the antibody. Sections were washed in TBS and incubated in the second antibody (biotinylated anti-rabbit 1:400 in SUMI) for 1 h at room temperature (RT). After washing in TBS sections were incubated for 1 h at RT in avidine biotinylated complex (1:800 in SUMI; Vector Laboratories, Burlingame, CA) for 1 h at RT and

 © 2012 Elsevier GmbH. All rights reserved.

MOLECULAR METABOLISM

Subject no.	Sex	Age	Diabetes/Control	Cause of death, clinical diagnoses, antidiabetic medication
98198	M	65	Control	Myocardial infarction, anemia, COPD, bronchus carcinoma, rib fracture
00007	M	85	Control	Myocardial infarction, PTCA
01005	F	76	Control	Respiratory insufficiency, Non-Hodgkin lymphoma
99046	F	89	Control	Myocardial infarction, heart failure, mitral valve insufficiency
01021	M	82	Control	Myocardial infarction, unsuccessful resuscitation, atrial fibrillation, heart failure, cataract
98095	M	75	Control	Respiratory insufficiency, pneumonia, COPD, atrial fibrillation, ischemic heart disease, mycosis fungoides
00072	M	78	Control	Renal insufficiency, atrial fibrillation, heart failure, dehydration
00006	F	26	Control	Respiratory failure, tonsillar hypertrophy, epilepsia
97146	F	100	Control	Pneumonia, tibia and fibula fracture
10013	M	70	Control	Pulmonary embolism, adenocarcinoma
97065	F	74	Control	Renal insufficiency, heart failure
82019	M	83	Type 2 Diabetes	Myocardial infarction, CVA, pneumonia, osteosynthesis for collum fracture, tolbutamide, metformin
95016	F	86	Type 2 Diabetes	Heart failure, angina pectoris, nephropathy, retinopathy, tolbutamide
98056	F	83	Type 2 Diabetes	Respiratory insufficiency, colon carcinoma, cataract, arthrosis anemia, no data on medication
03054	M	67	Type 2 Diabetes	Cardiogenic shock, multi-organ failure, COPD, insulin, metformin
97088	M	78	Type 2 Diabetes	Pneumonia, CVA, gliclazide
02087	M	71	Type 2 Diabetes	Respiratory insufficiency, multi-organ failure, gliclazide
08054	F	92	Type 2 Diabetes	Heart failure, melanoma, cholecystolithiasis, hepatic steatosis, ileus, cataract
09091	M	84	Type 2 Diabetes	Adenocarcinoma
97060	M	65	Type 2 Diabetes	Myocardial infarction, heart failure
98127	M	56	Type 2 Diabetes	Myocardial infarction, atrial fibrillation, osteoarthritis, nephropathy, neuropathy, dyslipoproteinemia, alcohol abuse, splenectomy
98062	M	85	Type 1 Diabetes	Respiratory insufficiency, diabetes induced neuropathy, pneumonia, COPD, bronchus carcinoma, no data on medication
98080	F	72	Type 1 Diabetes	Respiratory insufficiency, COPD, heart failure, polyneuropathy, insulin

Table 1: Clinicopathological data for subjects included in human brain tissue study.COPD, Chronic obstructive and pulmonary disease; CVA, cerebrovascular accident; F, female; M, male; PTCA, percutaneous transluminal coronary angioplasty.

subsequently rinsed in TBS (2×10 min). Finally, sections were incubated in 0.5 mg/ml 3,3'-diaminobenzidine (Sigma) in TBS containing 0.2% ammonium nickel sulfate (BDH; Brunschwig, Amsterdam, The Netherlands) and 0.01% H_2O_2 (Sigma, USA) for approximately 15 min. The reaction was stopped in distilled water. The sections were dehydrated in graded ethanol series, cleared in xylene, and cover slipped using Permount (Fisher Scientific GmbH, Germany). The number of the DAB-Ni precipitated vessels in every 100th section containing the IFN was counted in frames of 2 mm^2.

Statistical analysis

In the mouse studies, all values are expressed as the mean $\pm$ SEM, and data were analyzed using two-tailed t-test. Statistical significance was set at $P < 0.05$. In the human brain study, all values were expressed as median (range), data were analyzed using nonparametric Mann-Whitney U test and statistical significance was set at $P < 0.05$.

RESULTS

Exposure to a high calorie diet triggers hypothalamic angiopathy in mice

FITC-albumin infusion into the general circulation via tail vein was taken up by the basal lamina of blood vessels and labeled the entire vasculature in the CNS. Following 18 weeks of exposure to HFHS diet, mice had developed obesity, glucose intolerance (data not shown) and a significant increase of FITC-albumin labeled vessel length (Fig. 1B) and vessel density (Fig.1D) in the ARC, when compared to SC diet-fed age-matched controls (Fig.1A, C, E&F). Following chronic exposure to HFHS diet, mice exhibited significantly more αSMA-ir blood vessels within the ARC than mice fed SC diet (Fig. 2A&B). Short-term exposure to HFHS diet (between 1 day and 3 weeks) did not cause that phenomenon (Fig. 2C), suggesting that more arteries and arterioles form in response to chronic exposure to HFHS diet. Chronic exposure to HFHS also increased the occurrence of multiple cytoplasmic vacuoles and intracellular edema in endothelial cells (Fig. 2E), suggestive of endothelial degeneration, when compared to mice on SC diet (Fig. 2D), although the increase of the degeneration of endothelial cells did not reach significance when compared to SC diet control (Fig. 2F). These observed phenomena are reminiscent of certain features of diabetic microangiopathy. Besides endothelial cells degeneration, we observed no thickening of the basement membranes or blood brain barrier (BBB) rupture by loss of tight junctions (Fig. 2D&E). Furthermore, there was no effect of chronic HFHS diet exposure on the occurrence of peri- and juxta vascular damage, and disintegration of the endothelial surface was only rarely observed.

Human type 2 diabetes is associated with hypothalamic hypervascularization

We determined αSMA-ir in the infundibular nuclei (IFN, equivalent to ARC of rodents, in an area of 2 mm^2 of the IFN) of patients with type 2 diabetes where glucose levels were controlled by insulin, in contrast to diabetic animals. We discovered a significant increase of αSMA-ir-positive vessels in the type 2 diabetic patients (median 18.75; range 9.5–36) as compared to controls (median 8.41; range 5–15) (Fig. 3A C). Furthermore, most of the lumen diameters in the IFN of diabetic human brain were less than 10 μm, confirming that these αSMA-ir positive vessels were precapillary arterioles. We also studied two patients with type 1 diabetes (controlled glucose levels), and interestingly, although preliminary, the data also suggested more αSMA-ir positive vessels in the IFN of type 1 diabetes patients when compared to controls (25 &19 vs. 9.79 ± 1.33).

 © 2012 Elsevier GmbH. All rights reserved.

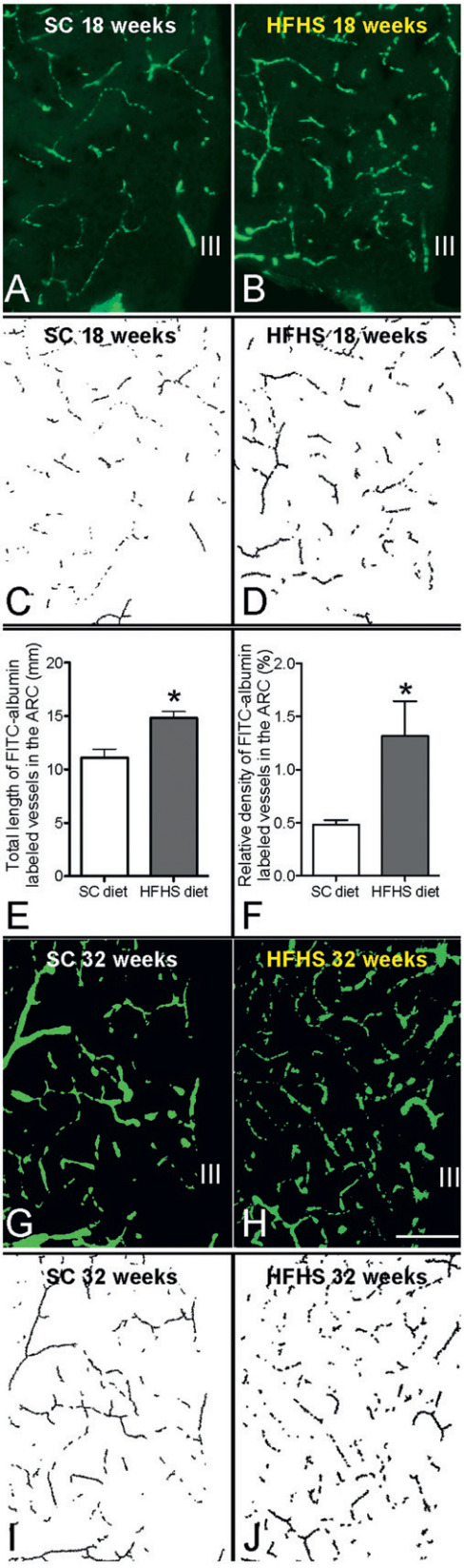


Fig. 1: Total vasculature in the ARC was labeled by FITC-albumin in mice fed 18 weeks of either standard chow (SC) diet (A) or high fat high sugar (HFHS) diet (B). The labeled images are skeletonized and shown in C and D. Quantification of the labeled vasculature reveals significantly increased total vessel length (E) and density (F) in the 18 week HFHS DIO mice compared to SC age matched controls. For comparison, total vasculature in the ARC was also labeled by FITC-albumin in mice fed 32 weeks SC diet (G) or HFHS diet (H). Although not quantified, the labeled images are skeletonized and shown in I and J.

DISCUSSION

Recent observations from several laboratories including our own suggest that hypothalamic processes beyond neuronal signaling may be involved in the pathogenesis of the metabolic syndrome. Pathophysiological observations of potential relevance following exposure to a hypercaloric environment include massive astrocytosis [9], prolonged microglial activation [9] and altered tanycyte function [16]. In addition, we observed IgG accumulation in the mediobasal hypothalamus [11], which suggests potentially impaired blood vessel permeability. In spite of an enormous focus on the neural circuitry of the mediobasal hypothalamus and its role in the control of systems metabolism, appetite and body weight, and in the pathogenesis of obesity and diabetes, we now report the occurrence of hypothalamic angiopathy, including neo- and hypervascularization, following chronic exposure to a high-calorie environment.

Supporting a role for the hypothalamic vascular system in the development of the metabolic syndrome we found increased vessel length and density as well as an increased number of degenerating endothelial cells within the ARC in mice following 18 weeks of HFHS diet. The number of arterioles was increased after 18 weeks but not after short-term exposure to HFHS diet (1 day–3 weeks). Furthermore, we found no other signs of diabetic microangiopathy or BBB breakdown (e.g., thickening of the basement membrane or loss of endothelial tight junctions). Hence, BBB leakage in response to HFHS diet is more likely to occur via direct toxic damage of endothelial cells than from an opening of endothelial cell contacts. An increase in artery and arteriole number was also found in the hypothalamic IFN of diabetic humans. Overall, these data suggest that chronic exposure to a hypercaloric environment and/or the resulting metabolic diseases (specifically diabetes) are causing a previously overlooked hypothalamic angiopathy syndrome. Future studies will have to investigate the extent to which such hypothalamic vascular pathology is causally relevant for the progression and ultimate irreversibility of impaired CNS metabolic control in late-stage obesity and diabetes.

In diabetic retinopathy, abnormal glucose metabolism and hyperglycemia-associated neo- and hypervascularization are hallmark features. Such vascular pathologies are known to cause neuronal damage in the retina and induce ocular hemorrhage-induced vision loss [17,18]. The retina is separated from the general circulation by the blood-retinal barrier (BRB), which in many ways, exhibits an ultrastructure similar to the BBB. Under hyperglycemic conditions, retinopathy begins with pathological changes of the pericytes, which wrap around the precapillary arterioles outside of the basement membrane. This is believed to be one of the major causes of blood-retinal barrier damage; the hyperglycemia persistently activates protein kinase C-δ, p38 and MAPK pathways, eventually leading to pericyte apoptosis [19]. Thereafter, vascular endothelial growth factor (VEGF or VEGFA) and Wnt signaling are among the key molecular underpinnings driving neovascularization in the retina [20]. We previously observed and reported a considerable increase of IgG infiltration in the ARC of mice on a high-calorie diet [11], indicating leakage of circulating macromolecules into the hypothalamus. Thus, in both the retina and the hypothalamus, BBB and BRB dysfunction and angiopathy appear to represent common features occurring in response to chronically impaired metabolic balance, including hyperglycemia, hyperlipidemia and insulin resistance. However, there appear to be some small, but important, differences in the pathogeneses of retinal and hypothalamic angiopathies. First of all, the key ultrastructural changes in the hypothalamic BBB are represented by degeneration of endothelial cells, but not

 © 2012 Elsevier GmbH. All rights reserved.

MOLECULAR METABOLISM

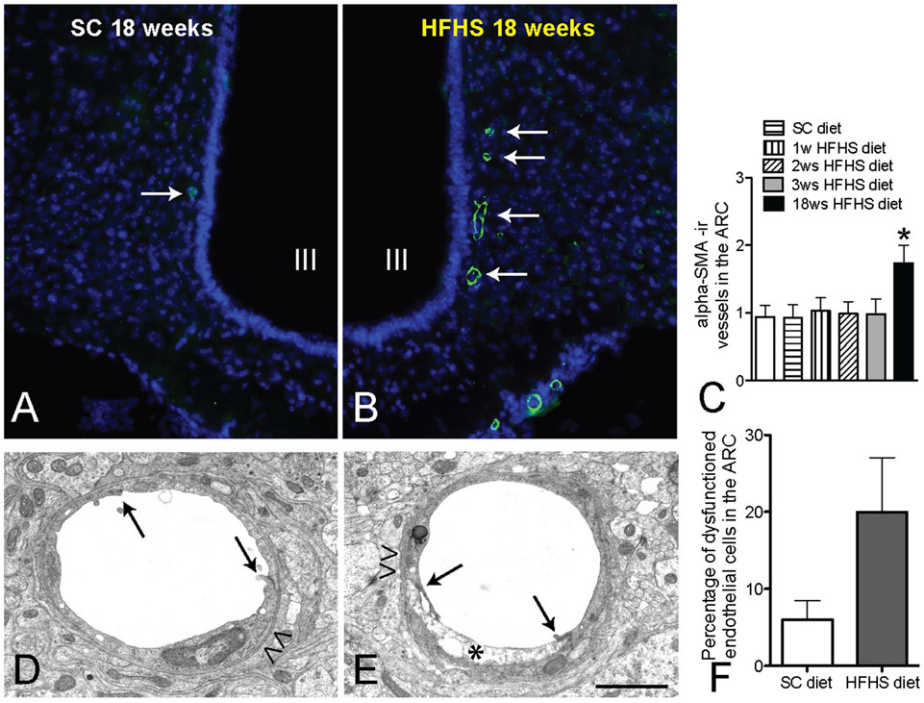


Fig. 2: After 18 weeks of HFHS diet, mice exhibit more αSMA-ir blood vessels (Green fluorescence, arrows in B) within the ARC than mice fed a SC diet (arrows in A); the ARC is visualized by DAPI staining (blue fluorescence). Ultrastructural analysis of the blood brain barrier after 18 weeks on HFHS diet reveals signs of endothelial degeneration (asterisk in E, F; difference did not reach significance), while tight junctions (arrows in D&E) and basement membranes (arrow heads in D&E) are intact in comparison to SC diet-fed controls. III: third cerebral ventricle. Scale bar: 120 μm in A & B, 1.5 um in D&E. (For interpretation of the references to color in this figure legend, the reader is referred to the web version of this article.)

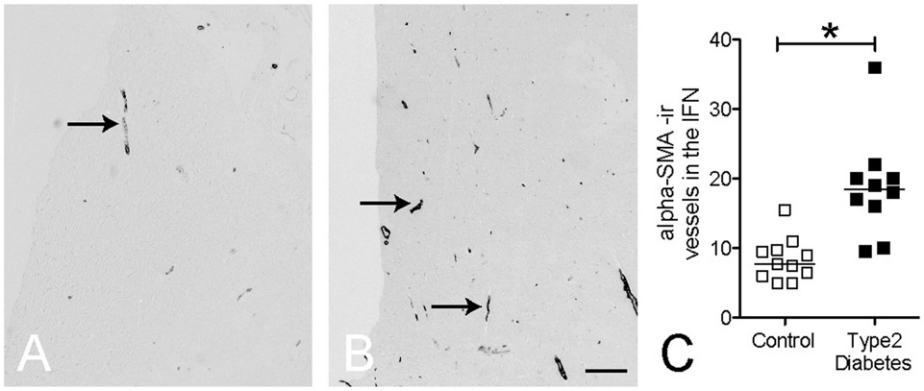


Fig. 3: Representative pictures of αSMA immunoreactivity in a patient with type 2 diabetes (B) and a matched control (A). A significant increase of αSMA immunoreactive vessel number was observed in diabetic patients hypothalamic infundibular nuclei (IFN), line indicates median value (C). Scale bar: 300 μm.

pericytes. This indicates that hypothalamic endothelial cells may be more susceptible to metabolic challenges as occurring during chronic exposure to a hypercaloric environment, which might lead to IgG infiltration. Second, we observed differences in the time course of IgG infiltration and angiogenesis within the ARC-ME area, with hypothalamic IgG infiltration preceding angiogenesis. In the pathogenesis of diabetic retinopathy, however, hemorrhagic events are likely the consequence, and not the cause, of neovascularization [21]. Further studies are underway to determine whether there are different types and time courses of macroprotein leakage in response to various specific metabolic challenges.

Previous studies in mice and rats by our lab and others have found that the immune-responsive cells such as ARC microglia are profoundly activated by exposure to high caloric diets. Such chronic activation likely impairs the physiological "cleansing" function of microglia, potentially even more so when the microglia are challenged with clearing high amounts of leaked IgG. In parallel, the enlarged end feet of activated astrocytes along the arterioles and capillaries could also lead to decreased nutrient and O_2 availability due to decreased penetration efficiency from the systemic circulation into the hypothalamic microenvironment. Finally, activated microglia and reactive astrocytosis both increase the metabolic activity within the local microenvironment. Consequently, the neural-glial network may have to initiate angiogenesis in order to obtain the required higher demand for nutrients and O_2. Interestingly, a recent study by other researchers has shown chronic cerebral hypoxia situation-induced angiogenesis, which also contributes to an increase of α-SMA-positive arterial vessels [22]. Whether HFHS diet induced hypothalamic angiogenesis is also caused by local hypoxia is a question that remains to be answered.

 © 2012 Elsevier GmbH. All rights reserved.

Angiogenesis entails a complex, synchronous process involving endothelial cells, supporting pericytes and vascular smooth muscle cells together with a plethora of molecular factors such as VEGF required to form new vessels [23,24]. A deeper understanding of the intricacies of these processes in the mediobasal hypothalamus is required to uncover pathogenic contribution to impaired CNS control circuitries in the metabolic syndrome.

In summary, our data reveal a previously unknown hypothalamic angiopathy or "hypothalangiopathy" syndrome. Hypothalangiopathy is triggered in rodent models by chronic exposure to HFHS diets, reminiscent of some features of diabetic retinopathy, and can be detected in the hypothalamus of diabetic patients as well. Ultrastructural alterations of the BBB ultrastructure indicate that prevention of endothelial cell degeneration might offer therapeutic strategies for the metabolic syndrome.

ACKNOWLEDGEMENT

This study is supported by Netherlands Organization for Scientific Research (NWO)-ALW-Rubicon (C.X.Y) and DFG-FOR1336 (I.B).

Conflict of interest. The authors declare no conflicts of interest.

REFERENCES

[1] Yi, C.X., Zeltser, L., and Tschop, M.H., 2011. Metabolic Syndrome ePoster—Brain & Neuron. Natural Medicine Supplements.

[2] Halaas, J.L., Gajiwala, K.S., Maffei, M., Cohen, S.L., Chait, B.T., Rabinowitz, D., et al., 1995. Weight-reducing effects of the plasma protein encoded by the obese gene. Science (New York, NY) 269:543–546.

[3] Friedman, J.M., 2009. Leptin at 14 y of age: an ongoing story. The American Journal of Clinical Nutrition 89:973S–979S.

[4] Halaas, J.L., Boozer, C., Blair-West, J., Fidahusein, N., Denton, D.A., and Friedman, J.M., 1997. Physiological response to long-term peripheral and central leptin infusion in lean and obese mice. Proceedings of the National Academy of Sciences of the United States of America 94:8878–8883.

[5] Levin, B.E., 2006. Metabolic sensing neurons and the control of energy homeostasis. Physiology and Behavior 89:486–489.

[6] Berthoud, H.R., 2008. The vagus nerve, food intake and obesity. Regulatory Peptides 149:15–25.

[7] Cottrell, G.T., and Ferguson, A.V., 2004. Sensory circumventricular organs: central roles in integrated autonomic regulation. Regulatory Peptides 117:11–23.

[8] Yi, C.X., Habegger, K.M., Chowen, J.A., Stern, J., and Tschop, M.H., 2011. A role for astrocytes in the central control of metabolism. Neuroendocrinology 93:143–149.

[9] Thaler, J.P., Yi, C.X., Schur, E.A., Guyenet, S.J., Hwang, B.H., Dietrich, M.O., et al., 2012. Obesity is associated with hypothalamic injury in rodents and humans. The Journal of Clinical Investigation 122:153–162.

[10] Horvath, T.L., Sarman, B., Garcia-Caceres, C., Enriori, P.J., Sotonyi, P., Shanabrough, M., et al., 2010. Synaptic input organization of the melanocortin system predicts diet-induced hypothalamic reactive gliosis and obesity. Proceedings of the National Academy of Sciences of the United States of America 107:14875–14880.

[11] Yi, C.X., Tschop, M.H., Woods, S.C., and Hofmann, S.M. (2012). High-fat-diet exposure induces IgG accumulation in hypothalamic microglia. Disease Models and Mechanisms.

[12] Skalli, O., Ropraz, P., Trzeciak, A., Benzonana, G., Gillessen, D., and Gabbiani, G., 1986. A monoclonal antibody against alpha-smooth muscle actin: a new probe for smooth muscle differentiation. The Journal of Cell Biology 103:2787–2796.

[13] Alkemade, A., Yi, C.X., Pei, L., Harakalova, M., Swaab, D.F., la Fleur, S.E., et al., 2012. AgRP and NPY Expression in the Human Hypothalamic Infundibular Nucleus Correlate with Body Mass Index, Whereas Changes in alphaMSH Are Related to Type 2 Diabetes. The Journal of Clinical Endocrinology and Metabolism 97:E925–933.

[14] Meijering, E., Jacob, M., Sarria, J.C., Steiner, P., Hirling, H., and Unser, M., 2004. Design and validation of a tool for neurite tracing and analysis in fluorescence microscopy images. Cytometry. Part A: The Journal of the International Society for Analytical Cytology 58:167–176.

[15] Herman, I.M., and D'Amore, P.A., 1985. Microvascular pericytes contain muscle and nonmuscle actins. The Journal of Cell Biology 101:43–52.

[16] Lee, D.A., Bedont, J.L., Pak, T., Wang, H., Song, J., Miranda-Angulo, A., et al., 2012. Tanycytes of the hypothalamic median eminence form a diet-responsive neurogenic niche. Nature Neuroscience 15:700–702.

[17] Bronson, S.K., Reiter, C.E., and Gardner, T.W., 2003. An eye on insulin. The Journal of Clinical Investigation 111:1817–1819.

[18] Willard, A.L., and Herman, I.M., 2012. Vascular complications and diabetes: current therapies and future challenges. Journal of Ophthalmology: 209538.

[19] Geraldes, P., Hiraoka-Yamamoto, J., Matsumoto, M., Clermont, A., Leitges, M., Marette, A., et al., 2009. Activation of PKC-delta and SHP-1 by hyperglycemia causes vascular cell apoptosis and diabetic retinopathy. Nature Medicine 15:1298–1306.

[20] Ruhrberg, C., 2003. Growing and shaping the vascular tree: multiple roles for VEGF. BioEssays: News and Reviews in Molecular, Cellular and Developmental Biology 25:1052–1060.

[21] Mohamed, Q., Gillies, M.C., and Wong, T.Y., 2007. Management of diabetic retinopathy: a systematic review. JAMA: The Journal of the American Medical Association 298:902–916.

[22] Boroujerdi, A., Welser-Alves, J.V., Tigges, U., and Milner, R. (2012). Chronic cerebral hypoxia promotes arteriogenic remodeling events that can be identified by reduced endoglin (CD105) expression and a switch in beta1 integrins. Journal of Cerebral Blood Flow and Metabolism: Official Journal of the International Society of Cerebral Blood Flow and Metabolism.

[23] Gerhardt, H., 2008. VEGF and endothelial guidance in angiogenic sprouting. Organogenesis 4:241–246.

[24] Montero, J.A., Ruiz-Moreno, J.M., and Correa, M.E., 2011. Intravitreal anti-VEGF drugs as adjuvant therapy in diabetic retinopathy surgery. Current Diabetes Reviews 7:176–184.

 © 2012 Elsevier GmbH. All rights reserved.